IOSR Journal of Environmental Science, Toxicology and Food Technology (IOSR-JESTFT)
e-ISSN: 2319-2402, p- ISSN: 2319-2399.Volume 20, Issue 5 Ser. 1 (May 2026), PP 84-99
www.iosrjournals.org

Adsorption Of Malachite Green Dye And Rhodamine B Dye By Use Of Activated Charcoal Prepared From Sunflower Seed Shell And Used Black Tea

Nazneen J. Shaikh, Sohail B., Dr. Khursheed A., Dr. Shaikh Kabeer Ahmed*
Assistant Professor,Post Graduate And Research Centre, Abeda Inamdar Senior College, Savitribai Phule University Pune, India.
Assistant Professor, Abeda Inamdar Sr. College, Pune.
HOD, Professor, Abeda Inamdar Sr. College, Pune PG Department Of Chemistry
PG Department Of Chemistry, Sir Sayyed Of Arts, Commerce and Science, Babasaheb Ambedkar University, Aurangabad, India.

Abstract:
A low-cost adsorbent was prepared from sunflower seed shells and used black tea (UBT) leaves for adsorption of malachite green dye (MG) and Rhodamine B dye (RhB) from aqueous solution. The tea leaves and sunflower seed shells (SSS) were used as precursors for the preparation of Activated charcoal (AC) in the present study. The prepared charcoal was activated by using the H_2SO_4 activation method, which involves a self-generated atmosphere using an oven (temperature at 600 °C). The characteristic of AC was determined by Fourier transform infrared spectroscopy, (FTIR) and observed by Scanning electron microscopy (SEM). SEM indicated that the surface of activated charcoal shows that surface is porous. The adsorption equilibrium and kinetics of malachite green (MG) and Rhodamine (RB) on activated charcoal were examined at 300K. The removal efficiency was tested with respect to adsorbent dose, P^H, time, concentration of adsorbent etc. Further experimental data was analysed to study the Langmuir, Freundlich and Temkin adsorption isotherm. The kinetics of sorption was well correlated using the pseudo-first order, second order rate equation and the intraparticle diffusion was involved.

Keywords: *Adsorption, malachite green (MG), Rhodamine B dye (RhB), activated charcoal, Used Black tea (UBT), Sunflower seed shell*

Date of Submission: 21-05-2026 Date of Acceptance: 31-05-2026

Fig 1: Adsorption of dyes on charcoal prepared from used black tea and Sunflower Seed Shell Adsorption of Melchite green and Rhodamine B on activated charcoal of Used Black tea and Sunflower seed shell

I. Introduction:

Industrial wastewater is a major environmental pollutant. Coloured wastewaters are produced in many industries, including textile, pharmaceutical, food, cosmetic, and leather [1]. Typically, the main pollutant in textile wastewater is organic dyes, many of which are resistant to biodegradation. Moreover, coloured wastewater prevents sunlight from penetrating the water and slows the rate of photosynthesis. Synthetic dyes are extensively used in paper, textile, food, and pharmaceutical industries. About 40,000–50,000 tons of dyes are continuously entering the water systems due to improper processing and dyeing methods from these industries [4]. The dyes are difficult to decolorize due to their complex structure, and most of the dyes contain aromatic rings, which make them mutagenic and Carcinogenic [8]

Dyes are widely used in the textile industry to colour products. A significant issue in textile wastewater is the presence of colored effluent. This wastewater contains diverse organic compounds and toxic agents, posing hazards to fish and aquatic organisms [10]. Malachite green and Rhodamine dyes are cationic dyes employed as food additives, dyestuffs, and, controversially, antimicrobials in agriculture. These dyes are applied to substrates such as silk, leather, and paper. Despite its name, malachite green is not derived from the mineral malachite. Malachite green (MG) causes serious eye burns and can lead to permanent injury in both humans and animals. Inhalation can trigger brief episodes of rapid or labored breathing, and ingestion results in burning sensations, nausea, vomiting, profuse sweating, confusion, painful urination, and methemoglobinemia [15]. These dyes endanger human and animal health. Therefore, eliminating color from wastewater is a key concern for environmentalists and researchers.

Over the years, the possibility of techniques such as oxidative degradation [17] have been exploited, but these methods possess drawbacks due to of their inapplicability to largescale units along with both energy and chemical intensiveness. Adsorption is a well-known and superior technique for dye and organic removal because of its easy operation, insensitivity to toxic substances, ability to treat concentrated forms of the dyes, and the possibility of reusing the spent adsorbent via regeneration.

In this work, In the present study activated carbon was prepared from low-cost adsorbent (Activated charcoal) like used black tea leaves and sunflower seed shell for the removal of Rhodamine B dye and malachite green from aqueous solution. The surface properties of applied adsorbent s were characterized by the methods like Infrared (IR) and scanning electron microscopy (SEM). The efficiency of adsorption process was analyzed based on the effect of different parameters such as P^H, contact time, adsorbent dose and initial dye concentration. Adsorption isotherm models (Langmuir and Freundlich), were used to analyzed the experimental data. The various kinetic models (Pseudo first order, pseudo second order, and intraparticle diffusion model) for the adsorption of dyes were carried out.

II. Material And Methods:

Activated Charcoal preparation:

To make activated carbon, the raw material used black tea (UBT namely Badshah Tea) was purchased locally, cleaned. The tea leaves were boiled with deionized water for at least 40 minutes. After boiling it is filtered and residue was dried in air for at least 3-4 days. Then the dried tea leaves and Sunflower seed cover were crushed, and ground in a food processor to a smaller particle size (1-2 mm). Then these dried tea leaves were impregnated with 2M H2SO4.(1:1, by weight) for 2days. Then filtered it with Whatmann filter paper and washed with water till pH neutral then dry the residue at normal condition for 2 days. After that Used black tea leaves and Sunflower seed shell was continuously stirred.

The mixture was dried in ovenafter being dehydrated overnight at 100°C.After cooling to room temperature, the activated product was rinsed with distilled water to get rid of any last traces of sulphuric acid until the water's barium chloride test revealed no sulphate. After drying the leaves and sunflower seed shell were kept in muffle furnace for 2 hours 5000C. After cooling it is used for adsorption process.

Rhodamine B **Melachite green dye**

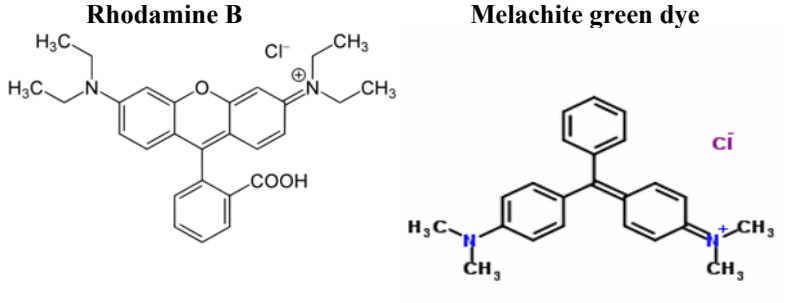

Fig2 Structure of Rhodamine B **Fig3: Structure of Malachite green**

Table 1: Some characteristic of the azo dyes methylene blue and Rhodamine B

Dye	Melachite green	Rhodamine B
Chemical class	cationic dye	Cationic dye
CAS number	569-64-2(chloride salt)	81-88-9
Colour Index number	42000	45170
Molecular formula	$C_{23}H_{25}ClN_{2(chloride)}$	$C_{28}H_{31}ClN_2O_3$
Molecular weight	364.911 g/mol (chloride)	479.01 g mol^{-1}

Preparation of stock solution: 1000mgL^{-1} of Melachite green dye (364.91) were prepared from by dissolving and 0.364g of A.R grade in double distilled water. The sample concentrations ranging from 10-100mgL^{-1} were prepared by diluting the stock solution to required concentrations Rhodamine B (RB) ($C_{28}H_{31}ClN_2O_3$; HPLC grade, M_r 479.01 g mol^{-1}), with a purity of 95% dye content, was purchased from Sigma-Aldrich and used without further purification. RhB stock solution was prepared by dissolving appropriate amount of dye powder in distilled water, and lower dye concentrations were obtained by diluting the stock solution.

Characterization of activated charcoal:

FTIR and FESEM analysis:

InfraRed spectroscopy provides qualitative information of characteristic functional groups on the surface of activated charcoal. The charcoal FTIR and SEM were taken from central Instrumentation Facility, Savitribai Phule University, Pune. The FESEM has Ultra High Resolution low voltage imaging and unique low vacuum capabilities. Its Resolution:1.0 nm at15kV, 1.4 nm at 1kV &1.8 nm at 3kV and 30Pa. In-lens TLD, SE and BSE detection.

The characterization of same activated charcoal was reported in the previous in terms of zero-point charge (pHpze), FTIR and SEM analysis.

Table No. 2 Interpretation of spectra for activated charcoal prepared from UBT

IR Frequency (cm^{-1})	Bond	Alcohol, phenol
3857.9	O-H Free stretching vibrations	Alcohol, phenol
3740.26	O-H stretching vibrations	Amine
3623.59	N-H stretching vibrations	Nitrile
2361.41	CN	Alkyne
2336.34	−C≡C−	Amide
1647.88	C=O stretching	Nitro group
1513.85	N-O stretching	Alkanes
1393.32	C-H bending	Aromatic or Alkene
673.999	Double bond C-H bending	Alkyl halide
574.683	C-Cl stretching	Alkyl halide
514.991	C-Br stretching	Alkyl halide

Figure illustrate FTIR spectra of Acctivated Charcoal Prepared from UBT .

Fig: 4 FTIR of Activated Charcoal prepared from used UBT:

Fig 4: FTIR of activated charcoal of UBT after adsorption of Rhodamine B dye

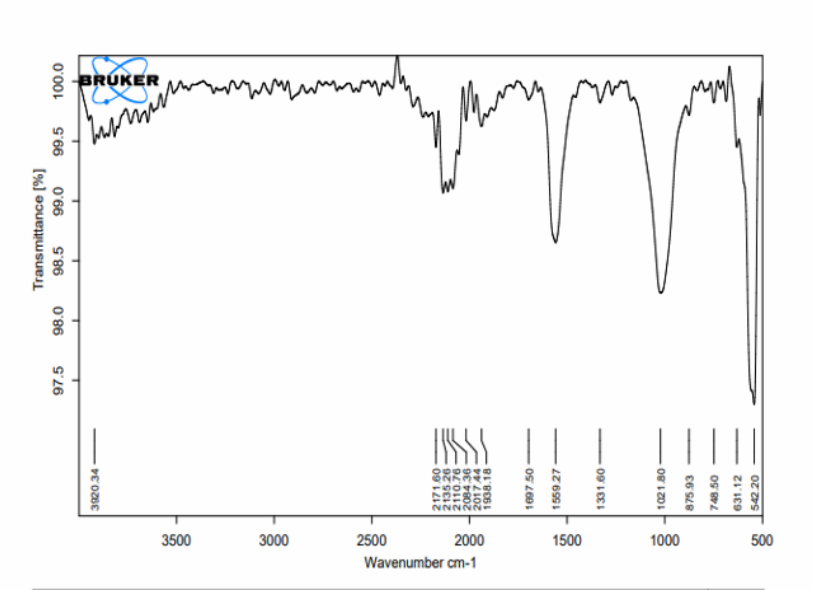

Fig 5: FTIR of activated charcoal of UBT before adsorption:

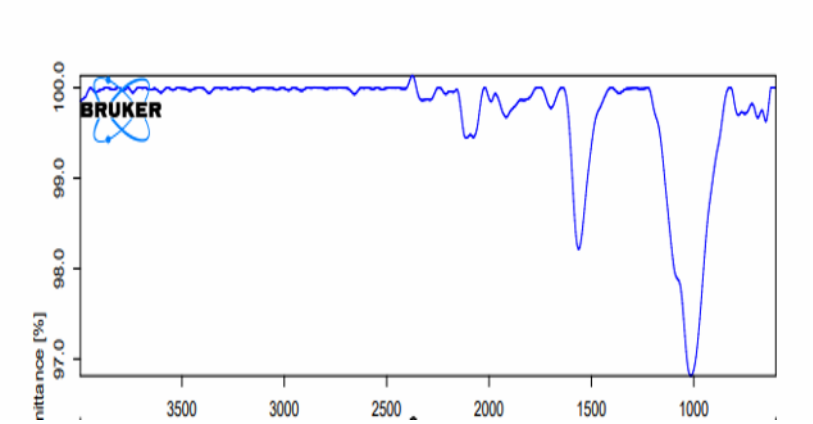

Interpretation of FTIR before Adsorption:

To determine the surface functional groups in charge of dye adsorption and to comprehend the adsorption mechanism, the FTIR spectra of UBT before and after Rhodamine B dye adsorption were examined.

The FTIR spectra of UBT before and after adsorption of Rhodamine B dye were analyzed to identify the surface functional groups responsible for dye adsorption and to understand the adsorption mechanism. The spectrum of UBT before adsorption shows several characteristic peaks corresponding to oxygen-containing functional groups commonly present in carbonaceous adsorbents.

A broad absorption band observed around **3200–3500 cm $^{-1}$** is attributed to the stretching vibration of hydroxyl (–OH) groups of alcohols and phenols. Similar observations have been reported for activated carbon and biomass-derived adsorbents, where hydroxyl groups play an important role in adsorption through hydrogen bonding and electrostatic interactions (Foo and Hameed, 2012; Gupta and Suhas, 2009).

The absorption band observed in the 2920–2850 cm $^{-1}$ region is attributed to C–H stretching vibrations associated with aliphatic chains, a feature that aligns well with FTIR spectral characteristics documented in the literature for biochar and activated carbon materials The band appearing in the 1600–1650 cm $^{-1}$ region is attributed to aromatic C=C stretching vibrations, with a possible contribution from carbonyl C=O stretching, suggesting the existence of conjugated aromatic frameworks within UBT. Comparable spectral features have been documented in activated carbons derived from agricultural residues, further corroborating the aromatic carbon nature of the material [5]. The peak at **1400–1450 cm $^{-1}$** corresponds to O–H bending vibrations or C–H deformation, while the band around **1000–1200 cm $^{-1}$** is attributed to C–O stretching vibrations of alcohol, phenol, and ether groups. These oxygen-containing functional groups are known to enhance adsorption capacity by providing active binding sites. Following Rhodamine B dye adsorption, notable alterations in peak intensities accompanied by marginal shifts in peak positions were evident in the FTIR spectrum. A reduction in intensity along with a slight positional shift of the hydroxyl (–OH) stretching band indicated its active participation in the adsorption mechanism. Analogous spectral shifts post-Rhodamine B adsorption have been documented in

earlier investigations, substantiating the contribution of hydroxyl groups to dye binding via hydrogen bonding interactions (Mittal et al., 2010). Furthermore, modifications observed in the bands associated with aromatic C=C and carbonyl (C=O) functionalities point toward π–π interactions between the aromatic framework of Rhodamine B and the aromatic surface of the adsorbent. Such interaction mechanisms have been extensively cited in the literature as the predominant pathway governing Rhodamine B adsorption onto carbon-based materials[53]. Following Rhodamine B dye adsorption, notable alterations in peak intensities accompanied by marginal shifts in peak positions were evident in the FTIR spectrum. A reduction in intensity along with a slight positional shift of the hydroxyl (–OH) stretching band indicated its active participation in the adsorption mechanism. Analogous spectral shifts post-Rhodamine B adsorption have been documented in earlier investigations, substantiating the contribution of hydroxyl groups to dye binding via hydrogen bonding interactions (Mittal et al., 2010). Furthermore, modifications observed in the bands associated with aromatic C=C and carbonyl (C=O) functionalities point toward π–π interactions between the aromatic framework of Rhodamine B and the aromatic surface of the adsorbent. Such interaction mechanisms have been extensively cited in the literature as the predominant pathway governing Rhodamine B adsorption onto carbon-based materials [53]

Additionally, the modifications noted in the C–O stretching region further validate the involvement of oxygen-containing functional groups in the adsorption process. The binding of dye molecules onto the UBT surface is likely governed by a combination of electrostatic attraction, hydrogen bonding, and π–π interactions, a mechanistic pattern that is in accordance with adsorption behaviors previously established for cationic dyes on activated carbon and biochar-based adsorbents.

FTIR peak comparison of UBT before and after adsorption of Rhodamine B dye

The FTIR spectra of UBT before and after adsorption of Rhodamine B dye show noticeable shifts in peak position and changes in intensity, confirming the involvement of surface functional groups in the adsorption process. The comparison of peak values is presented in Table below.

Table 3: FTIR peak values before and after adsorption of Rhodamine B onto UBT Functional group :

Fuctional group	Peak before adsorption (cm^{-1})	Peak after adsorption (cm^{-1})	Interpretation
–OH stretching (hydroxyl	3420	3405	Shows involvement of hydroxyl group in hydrogen bonding with Rhodamine B
C–H stretching (aliphatic)	2922	2915	It shows contact between dye molecules and carbon surface
C=O stretching / Aromatic C=C	1630	1620	Shows π–π interaction between Rhodamine B aromatic ring and UBT surface
O–H bending / C–H bending	1425	1418	Confirms participation of surface functional groups in adsorption
C–O stretching	1105	1092	Shows involvement of alcohol, phenol, or ether groups
Aromatic C–H bending	-	868	Interaction of dye and aromatic structure

Interpretation of FTIR after adsorption of dyes:

The FTIR spectrum of activated charcoal of UBT before adsorption shows characteristic peaks corresponding to hydroxyl, carbonyl, aromatic, and ether functional groups. After adsorption of Rhodamine B dye, shifts in peak position and reduction in intensity were observed. The hydroxyl peak shifted from 3420 cm^{-1} to 3405 cm^{-1}, indicating hydrogen bonding between dye molecules and hydroxyl groups on the UBT surface. Similarly, the peak at 1630 cm^{-1} shifted to 1620 cm^{-1}, confirming π–π interaction between the aromatic structure of Rhodamine B and the carbon surface.

The C–O stretching peak also shifted from 1105 cm^{-1} to 1092 cm^{-1}, indicating involvement of oxygen-containing functional groups in adsorption. These shifts confirm that hydroxyl, carbonyl, and aromatic functional groups play an important role in Rhodamine B adsorption.

Such peak shifts after dye adsorption have also been reported in previous studies, confirming that adsorption occurs through hydrogen bonding, electrostatic interaction, and π–π interaction between dye molecules and adsorbent surface functional groups.The FTIR spectrum of UBT before adsorption displays distinct peaks for hydroxyl, carbonyl, aromatic, and ether groups. After Rhodamine B dye is adsorbed, these peaks shift and their intensity decreases. The shift of the hydroxyl peak from 3420 cm^{-1} to 3405 cm^{-1} suggests hydrogen bonding between the dye and UBT. The 1630 cm^{-1} peak moving to 1620 cm^{-1} indicates π–π interactions with the dye's aromatic structure. The change in the C–O stretching peak from 1105 cm^{-1} to 1092 cm^{-1} shows oxygen-containing groups are also involved. These observations highlight the role of aromatic, carbonyl, and hydroxyl groups in adsorption. Previous studies have observed similar peak shifts, confirming adsorption via hydrogen bonding and electrostatic interactions

Fig 6: FTIR of Activated charcoal before and after adsorption Sunflower seed shell:
Fig 6:(a) and (b)

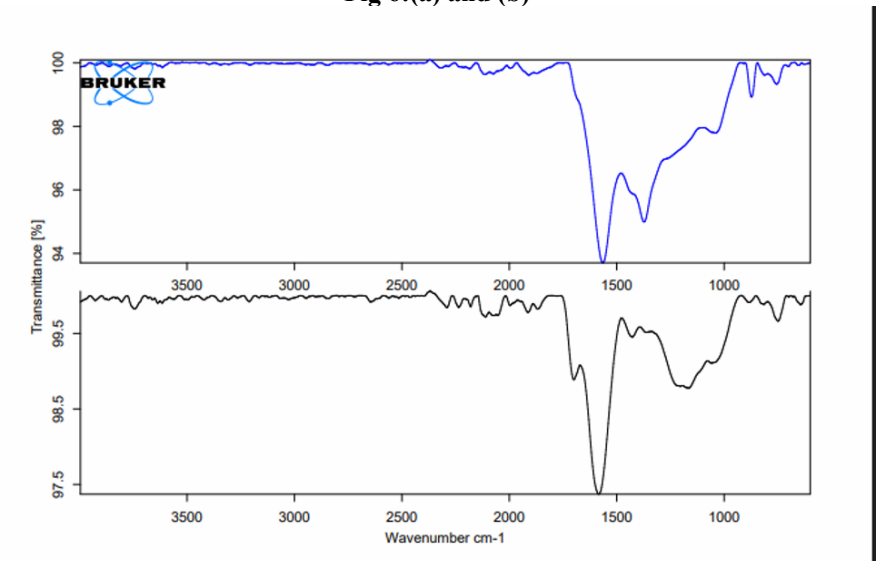

Table 4: FTIR Spectrum Before Adsorption (Raw/Activated Charcoal):

Wavenumber (cm ^{1})	Functional Group (before adsorption)	Interpretation
3200–3500	**–OH stretching**	**Hydroxyl groups (alcohols/phenols), hydrogen bonding**
2920–2850	**C–H stretching**	**Aliphatic hydrocarbons**
~1700–1730	**C=O stretching**	**Carboxylic acids, esters, lactones**
~1600–1650	**C=C / aromatic**	**Aromatic ring vibrations / conjugated carbon**
1400–1450	**C–H bending**	**Aliphatic deformation**
1000–1200	**C–O stretching**	**Alcohols, ethers, phenols**
600–800	**Functional Group**	**Out-of-plane bending**

The FTIR spectrum of sunflower seed shell activated charcoal typically shows the presence of various oxygen-containing functional groups responsible for adsorption.

Interpretation before adsorption shows presence of –OH, C=O, and C–O groups indicates active adsorption sites. These functional groups contribute to metal ion binding via ion exchange, complexation, and electrostatic Figure illuatrte FTIR spectra of UBT. FTIR figure shaows a large number of peaks due to adsorption. The broad peak form 3857.9cm-1 represent -OH (hydroxyl) functional sgroups on UBT free streching vibration. The strong peaks from 2361.41 is evidence of CN. The strong absorption peak at 1647.88Cm-1 is attributed to the presence C=Obond. The vibration at 2336.34 is due to presnece of −C≡C− (amide). The bond at 1513cm-1 is due to N-O streching . The peak at 1393.32cm-1 is due to presence of -CH bending .The bond at 673.99cm-1 foe double bond C-H bending . The peak fro 514cm-1 to 574cm-1 for alkly halide. These functional groups ar active for dyes removal . All the previous peaks shows a shift to a new wavelength, which is an indication of the participation of the functional in the adsorption process and as in the table. After adsorption (e.g., heavy metals or dyes), noticeable shifts and intensity changes occur.

Table 5: FTIR Spectrum After Adsorption:

Wavenumber (cm ^{1})	Functional Group (after adsorption)	Interpretation
~ 3400 cm ^{1}	–OH stretching	Shift to lower/higher wavenumber, reduced intensity Involvement in hydrogen bonding or metal coordination
~1700 cm ^{1}	C=O stretching	Complexation with dye
~1100 cm ^{1}	C–O stretching	Participation in adsorption
~1600 cm ^{1}	Aromatic C=C	Interaction with adsorbate molecules

After adsorption of malachite green dye at 3400cm^{-1}-OH stretching occurred due to this reduced intensity and hydrogen bonding had occurred. Similar observation had shown in biomass activated carbon for the study of Foo & Hameed (2012). Peak at 1700cm^{-1} after adsorption shows C=O stretching due to complexation with dye it has also shown by Babel & Kurniawan (2003), heavy metal adsorption, Shift in carboxyl and hydroxyl results from metal binding with oxygen, confirms active participation of oxygenated groups as the study on Agricultural Waste Adsorbents (Demibras, 2008). The FTIR analysis of sunflower seed shell activated charcoal reveals the presence of functional groups such as hydroxyl, carbonyl, and ether groups, which play a significant role in adsorption.

SEM Observation:
The pore size of charcoal for sunflower seed shell is nearly about 1.535µm and 8µ average.

Fig 7 : **SEM imges of Activated charcoal of Sunflower seed shell before adsorrption of MG**

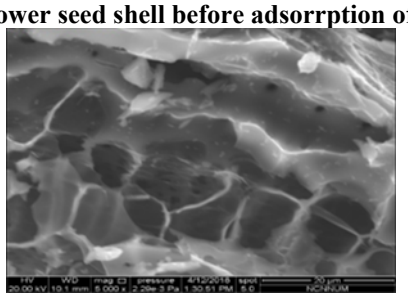

Fig8: SEM of Activated charcoal of Sunflower S.S. before adsorption of MG

Fig 9: SEM images Activated charcoal of Sunflower seed shell after adsorption

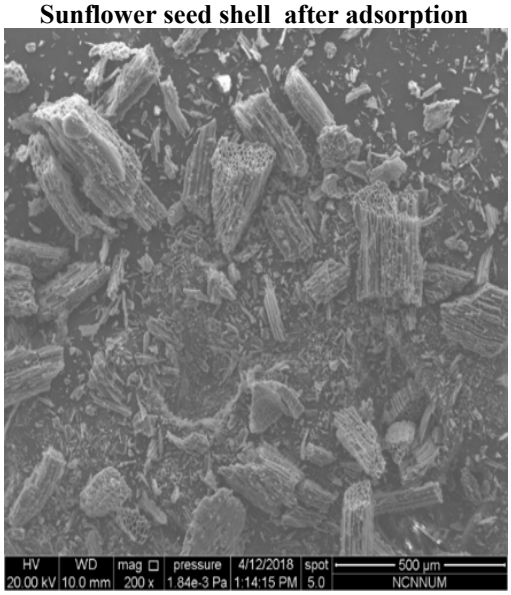

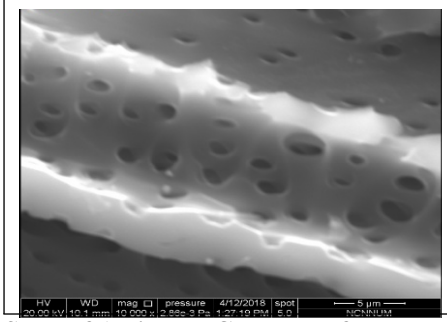

SEM of Activated Charcoal after adsorption of Rhodamine B dye

:

Fig 10 SEM of Activated charcoal of UBT before adsorption of RhB dye

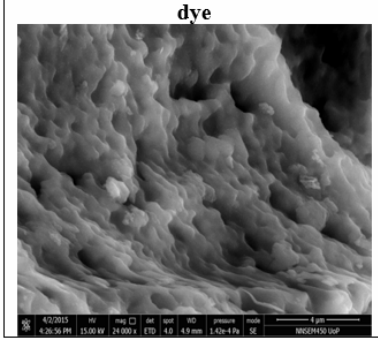

Fig11: SEM of Activated charcoal of UBT after adsorption of Rhodamine b

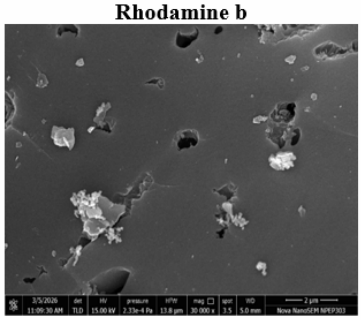

Fig 12: SEM of charcoal from UBTafter Rhodamine B dye adsorbed

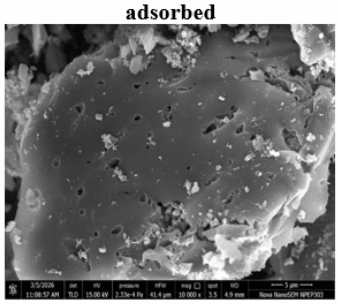

Adsorption experiment:

The equilibrium adsorption isotherm for removal of Rhodamine B dye and malachite green dye from aqueous solution. By using impregnated activated charcoal of used black tea has been investigated. Liquid phase adsorption experiment was conducted, and maximum adsorption capacity was determined. The effect of various parameters such as effect of adsorbent, effect of pH, effect of Contact time, and different adsorption isotherms were studied to optimize the condition of maximum adsorption. The Melachite green and Rhodamine B dye indicator having batch adsorption experiments were investigated. The high concentration of Rhodamine B and malachite green dye solution was significantly chosen to carry out our adsorption experiments as the initial concentration parameters. The concentration 10 mg/L to 100 mg/ L of Rhodamine B and malachite green dye aqueous solution was prepared in distilled water and these aqueous solutions were poured into a flask which contain accurately weighed amount of adsorbent that is activated charcoal. The activated charcoal was weighed in the range of 0.1 to 1g for 50 ml of malachite green solution, Rhodamine B dye. Then flask was continuously stirred by using magnetic stirrer for definite time to maintain equilibrium. This solution was centrifuge by using centrifuge machine. The absorbance of supernatant solution measure by calorimeter (Equiptronic model EQ 650A Colorimeter). The measurement was carried out at 298 k for malachite green and Rhodamine B dye absorbance was measured at wavelength 600nm (MG) and 540nm (RhB).

Effect of pH

For rhodamine B dye: Effect of pH for rhodamine dye and malachite green on activated charcoal prepared UBT was prepared and is given in the figure 16. Adsorption removal for rhodamine dye from pH 1 to 12 was detected %removal is higher at pH=12. For malachite green dye on sunflower seed shell was detected from pH 2 to 9. The pH -2 had shown a highest removable efficiency pH for MG from sunflower seed shell.

Fig 16: Effect of pH on MG and RhB :

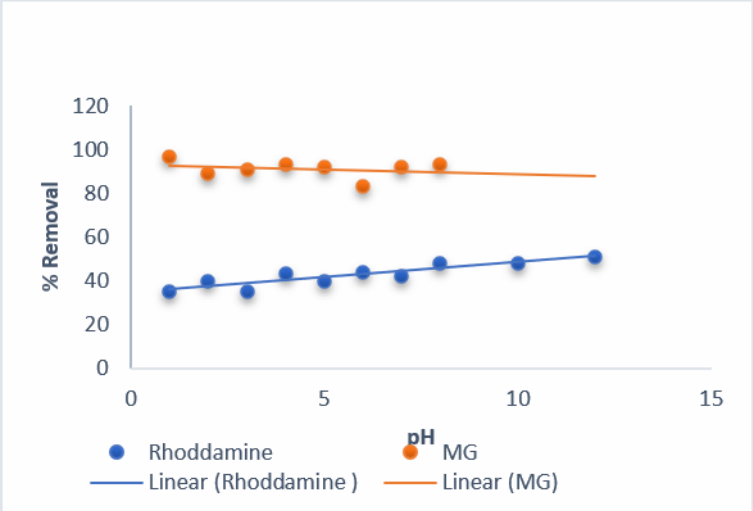

The effect of pH of rhodamine B and malachite green dye on activated charcoal showed adsorption capacity significantly increased from 60% to 96%at p.The high The initial high adsorption rate may have been due to high driving force accelerating molecules to the surface of activating charcoal and interacting with numerous active sites. The decrease in the adsorption may be attributed to decreased number of active adsorption site and long-range diffusion effect of molecules. The equilibrium adsorption capacity was reached up to 2 hours.

Fig 17: Effect of time on MG and RB:

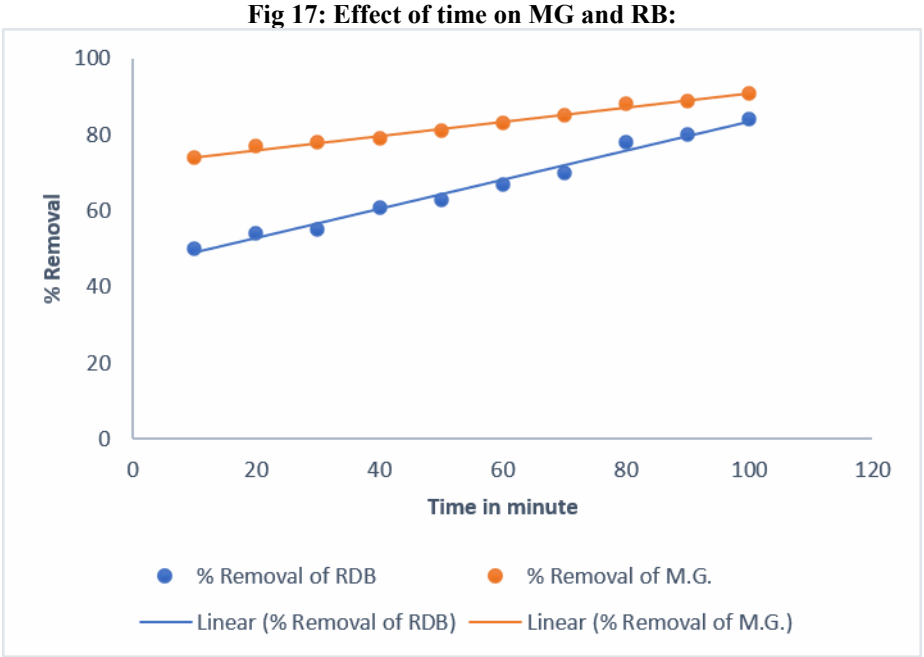

Effect of time:

The effect of time MG and Rhodamine B on activated charcoal was observed from 20–120minute adsorption equilibrium was reached. The high adsorption rate was observed for sunflower seed shell as compare for UBT. The effect of contact time for RDB (50ppm) and MG (50ppm) on activated charcoal adsorption capacity significantly increased from 10 to 100 minutes adsorption equilibrium was reached. The initial high adsorption rate may have been due to high driving force accelerating molecules to the surface of activating charcoal and interacting with numerous active sites. The decrease in the adsorption may be attributed to decreased number of active adsorption site and long-range diffusion effect of molecules. The equilibrium adsorption capacity was reached up to 2 hours. Further increase in contact time does not increase the uptake due to deposition of dyes on the available adsorption site on charcoal.

Fig 18: Effect of adsorbent:

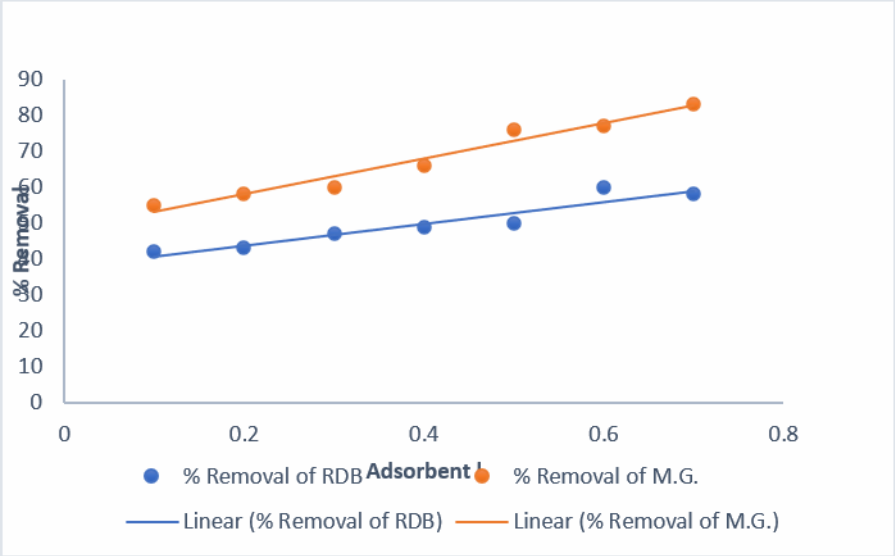

Effect of adsorbent:

The effect of adsorbent dose on the removal ratios for MG and rhodamine dyes are shown in the fig**.18** The percentages of dyes adsorbed increased as the adsorbent dose was increased from 0.1- 1.0g per 50ml. The adsorption of dyes increases from 55% to 82% for malachite green dye and 42%to 60% for Rhodamine dye using activated charcoal**.** An increase in adsorption with higher sorbent dose results from expanded surface area and enhanced availability of adsorption sites. This trend corresponds with the Langmuir hypothesis, which posits increased competition among sorbent particles for organic compounds as their concentration per unit volume rises. So, in other parameter experiments, adsorbent amount of 0.1g per 50ml was chosen.

Effect of Zeropoint charge:

Fig:19 Effect of zeropoint charge for malachite green on activated charcoal from sunflower seed shell

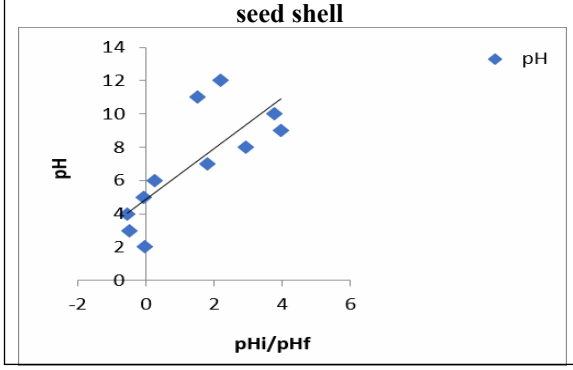

Fig 20: Effect of Zeropoint charge for RhB on activated charcoal of UBT

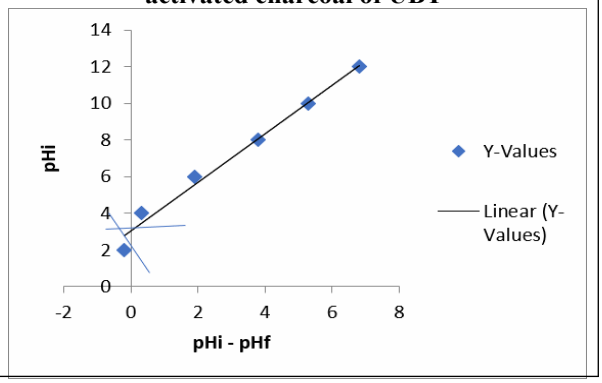

The pH at point of zero charge (pH-pze) on the surface of prepared activated carbon was found to be 3.6 for UBT and 5.0 for sunflower seed shell (Fig19 & 20). The UBT charcoal exhibits a relationship between the point of zero charge (pH-pze) and the adsorption capacity of the adsorbent used. The results indicate that cation adsorption is favourable at pH values higher than the point of zero charge, while anion adsorption is favoured at pH values lower than the point of zero charge [23-25]. This suggests that when the pH is less than the pH-pze, adsorption is more favourable due to the strong electrostatic attraction between anionic dyes and the protonated oxygen-containing surface functional groups on the activated charcoal. Conversely, at pH values greater than the pH-pzc, the adsorption of malachite green and Rhodamine -B dye is more favourable due to the strong electrostatic attraction between cationic dyes and the negatively charged surface functional groups on the activated charcoal.

Adsorption equilibrium study:

Equilibrium data, commonly known as adsorption isotherms, are basic requirement for the design of adsorption systems. To discover the adsorption capacity of activated carbon prepared from tea leaves, the experimental data points were fitted to Langmuir and Freundlich isotherm equation 5 and 6 and the constant pa

Langmuir isotherm.

The Langmuir equation relates to the coverage of molecules on a solid surface to concentration of a medium above the solid surface at a fixed temperature. This model assumes **monolayer** adsorption, where adsorption can occur at definite sites. The Langmuir equation can be written in the following form (Zhang et.al.2009; Chiou and Li2002; Langmuir1918):

----------(3)

parameter of these equations were calculated (Fig 11and 12).

Where, Ce (mg L^{-1}) is the equilibrium concentrations of RhB and UBT (mg/L), q_e, the amount of adsorbate per unit mass of adsorbent (mg g^{-1}), K_L is the Langmuir constant (Lmg^{-1}) and q_m is the amount of adsorption corresponding to maximum adsorption capacity (mg g^{-1}). The value of q_m is recognized as the adsorption capacity, which is commonly a measure of adsorption ability of an adsorbent. K_L and qm are determined from intercept and slope of linear plot of 1/qe and 1/Ce

The shape of Langmuir isotherm was calculated from the dimensionless constant called separation factor R_L (Zhange et.al.,2009, Kinniburgh,1986; Gupta et al.,2013; Mittal et al., 2016)

A dimensionless constant R_L known as separation factor defined by Webber and Chakravorti was used to calculate the shape of the Langmuir isotherm (Zhange et al., 2009, Mittal et al., 2016)

$R_L = 1/ 1+K_LCi$

Where C_i is the initial concentration, and K_L is the Langmuir constant. The value of R_L indicates the type of isotherm. If the value of R_L=1, it indicates linear isotherm. If the value of R_L=0 it indicates isotherm to be irreversible, if the value lies ($O < R_L < 1$) it indicates favourable isotherm, $R_L > 1$ it is unfavourable.

When Ce/q_e was plotted against Ce straight line with slope $1/q_m$ was obtained (Fig.21and Fig 22.) indicating that adsorption of RDB and MG on activated carbon prepared from sunflower seed shell and used black tea leaves (UBT) follow the Langmuir isotherm. The maximum adsorption capacity q_m for complete monolayer coverage of RDB and MG is found to be 97. 16mg/g and 222.22 mg/g.

Fig 21. Langmuir isotherm plot of MG(50ppm) on sunflower seed shell (50ppm) :

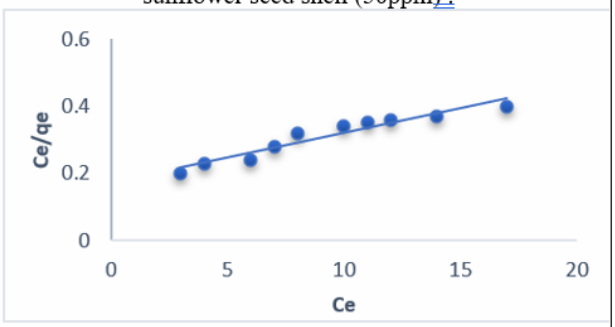

Fig22: Langmuir isotherm plot of MG on Sunflower seed shell(100ppm)

Fig 23. Langmuir isotherm plot of Rhodamine B on UBT

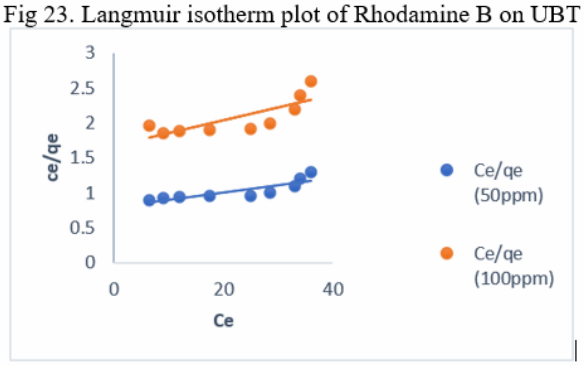

Fig 25 Freundlich isotherm for MG on sunflower seed shell for 100ppm

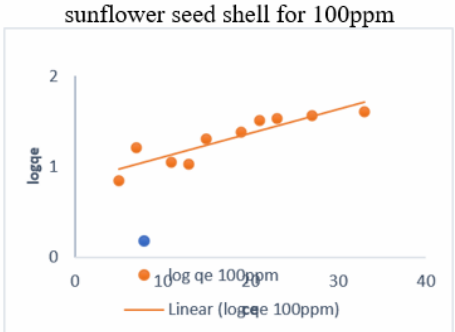

Freundlich Adsorption Isotherm:

The Freundlich equation was developed mainly to allow for an empirical account of the variation in adsorption heat with concentration of an adsorbate (vapor or solute) on an energetically heterogeneous surface.

(5)

where is the mass of adsorbate adsorbed per unit mass of adsorbent (mg g^{-1}), is the equilibrium concentration of adsorbate (mg L^{-1}) for RDB and MG.

K_f indicates adsorption capacity and n an intensity factor of the adsorption process, which varies with the heterogeneity of the adsorbent.

The adsorption is more favourable when 1/n is greater. The fractional values of 1/n ranged between 0 and 1. The constant K_f and 1/n were calculated from the intercept and slope of the plot of logqe Vs logCe.

For Sunflower AC Charcoal:

The value of 1/n and the constants K_f were calculated from the intercept and slope of the plot of logVs.log. Figure 12 shows the linear plot of Freundlich isotherm for adsorption lies between 0 and 1 is a degree of adsorption intensity or surface heterogeneity, becoming more heterogeneous as its value gets closer to zero.

Fig 24: Freundlich isotherm for Sunflower seed shell

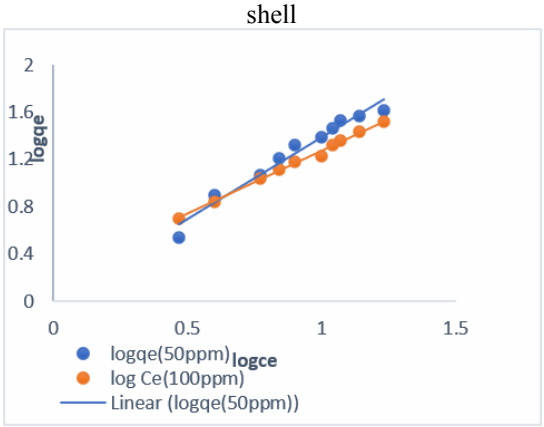

Fig 26: Freundlich isotherm For Rhodamine B dye

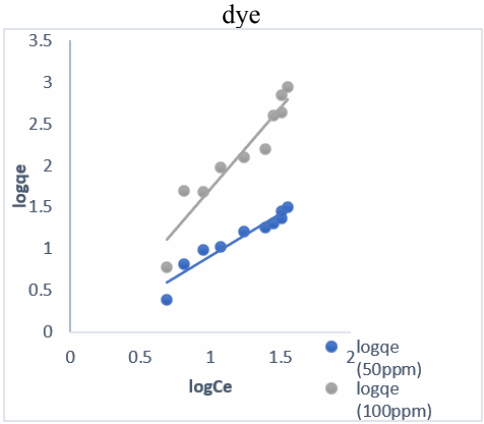

Temkin adsorption:

The linear form of Temkin isotherm is given by the equation

$q_e = B \log K_t + B \log C_e$

Where B =RT/b represent the heat of adsorption, T is the absolute temperature (K), R is the universal gas constant (J K^{-1} mol^{-1}), 1/b indicates the adsorption potential of the adsorbent and k_t (L mg^{-1}) is the equilibrium binding constant corresponding to the maximum binding energy.

The plot of q_e versus log C_e allows the determination of isotherm constants B (J mol^{-1}) and K_t (L m^{1})**.**

Fig: **Fig27: Temkin isotherm for MG (50ppm)**

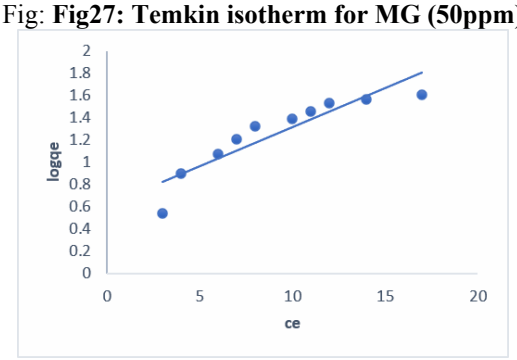

Fig: **Fig28: Temkin isotherm Rhodamine dye (100ppm)**

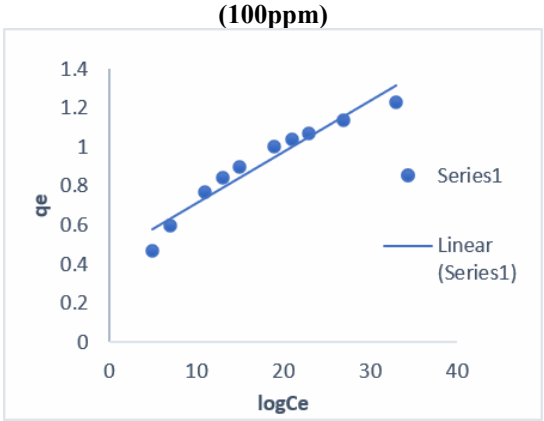

Fig: **Fig 29: Temkin adsorption isotherm Rhodamine B(50ppm)**

Fig28: Temkin isotherm Rhodamine dye (100ppm)

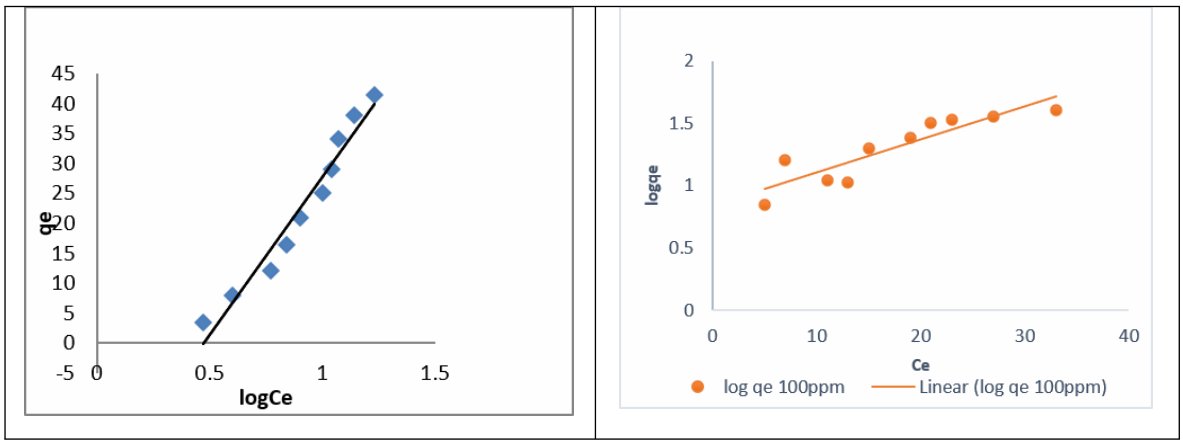

Table 7. Adsorption isotherms analyzed parameters.
Adsorption of MG and Rhodamine B dye on activated charcoal prepared from Sunflower seed shell and UBT.

Langmuir adsorption isotherm				Freundlich adsorption isotherm			Temkin adsorption isotherm		
Dye	K_L	$_{qm(mg/g)}$	R^2	K_f	n	R^2	B	K_t	R^2
Rhodamine B (100ppm)	91.94	54.94	0.62239	4.0485	0.5245	0.8032	2.552	294	0.9381
Rhodamine B (50ppm)	77.63	97.082	0..7226	8.613	0.975	0.9758	0.0262	0.2217	0.9571
Melachite green 50ppm	11.85	68.027	0.9278	2.44545	0.72020	0.9654	0.0699	77.81	0.8363
Malachite green 100ppm	206.13	222.22	0.5437	1.004616	0.0160	0.8151	0.0265	998.6	0.8083

Table 8: Comparison of the Rhodamine B dye and MG on different adsorbent

Adsorbent	qm(mg/g) Rhod. B	qm(mg/g) MG	Reference
UBT	97.082	-----	This study
Sunflower Seed		222.22	This study
PK-AC1	413.9	----	[1]
EAC2	281-389	----	[2]
Co/OMC3	879	----	[3]
Activated SDC4		183	
Activated RHC5		86.9	
C-AC 6	32-40		
Graphene	201-20		
Activated Carbon	85-250		
Activated carbon	102-114.68		
AC-MnO2-NC7	76.92		
PLAC8	500-560		
APTC9	307.2		
RPAC10		49-220	
PAN/AC11		217.39	
OMC	1028		
Activated white sugar	123.46		[3]
Corn Stalk	5.6		[ ]
Pericarp of rubber	0.298mmol/g		[ ]
Modified coir pith			[35]
Bakers' yeast	14.9		[36]
Cedar Cone	25		[38]
Sugarcane baggase	4.55		[37]
Acid treated montmorllonite	51.5		[34]
	188.67		[12]

Adsorption kinetics

The dye removal kinetics of Rhodamine B and malachite green dye on the surface of UBT and sunflower seed shell. Pseudo-first order, pseudo-second order and intra-particle diffusion models were used for characterizing the kinetics data [1]

Pseudo-first order kinetic model :

The data is subjected to Lagergren's first order equation. It has been found that it does not fit to straight line.

$dqt/dt = k_1(q_e - q_t)$ ---------- *5*

where k_1 is the pseudo-first -order rate constant(min-1); t is time of contact between the adsorbent and adsorbate (min); qe is the adsorption value after the equilibrium stabilization (mg/g); and qt is the adsorption value in given timet (mg/g) equation (6) in linear form

$\ln (qe-qt) = \ln qe-k_1*t.$ …… 6

The values of qe and $K_1$was found from the slope and intercept of the linear relation between log (qe-qt) with t at the given concentrations. The straight line between log(qe-qt) with 't' highlight the Eq.(6).

The rate constant were calculated from linear plots of $\ln(q_e - q_t)$ *versus t (data shown).*

$log(q_e - q_t) = log\ q_{el}$ …… 7

Pseudo-second order kinetic model

The integrated linear form of pseudo-second order kinetic model is given below

$t/q_t = 1/(K_2q_2e) + t$ ……8

where q_e is a MG or Rhodamine adsorbed onto the unit weight of adsorbent at equilibrium (mg/g), q_t is the MG or Rhodamine adsorbed onto the unit weight of adsorbent at any time t(mg/g) and K_2 is the pseudo-second order rate constant (g mg^{-1} min^{-1}) for second order model(L/min). For pseudo-second order kinetic model, the linear plot between *log (qe-qt)* verses *t*. The values of q_e, K_2 and R^2 was found from the slope and intercept of the linear relation between t/qt at concentrations. The straight line between t/qt and time emphasizes the applicability of equation (48) as shown in Fig.14. are listed in Table 4 shows each of the following parameters k_1, k_2, R^2at the given concentration for MG and Rhodamine B. The experimental data, qe, exp differ from theoretical values qe cal (Table 9), suggests that the adsorption of MG and Rhodamine B on activated carbon does not entirely follow the pseudo-first order adsorption kinetics.

The values of q_e shows that pseudo-first order model was obeyed for MG. The data also shows that the values of the determination coefficient (R^2) for the pseudo first order model were 0.9256 (100ppm) ,0.8979(50ppm) and first order model was not obeyed for Rhodamine B respectively. The plot of t/qt versus t gives an excellent straight line relation for adsorption of MG and on RB (Fig34 and Fig35). Whereas R^2 values for the pseudo second model were 0.9051(100ppm) for the MG and 0.9083(100ppm) Rhodamine B dye respectively. The higher regression coefficient R^2 values indicates that pseudo-first order model better fits for MG and pseudo-second order for RB. It can be seen in the table 9 that with an increase in dye concentration increase in the rate of adsorption is being observed. The pseudo second order rate constant of RB (1.3987 g mg^{-1} min^{-1}) was greater than pseudo first order rate constant (k_1) of MG (0.1821g mg^{-1} min^{-1}) and RB (0.0096726 g mg^{-1} min^{-1}). Which indicates that the rate of RhB adsorption on activated charcoal of used black tea was greater than MG adsorption.

Fig31: Melchite green dye adsorption on sunflower seed shell for first order kinetic study

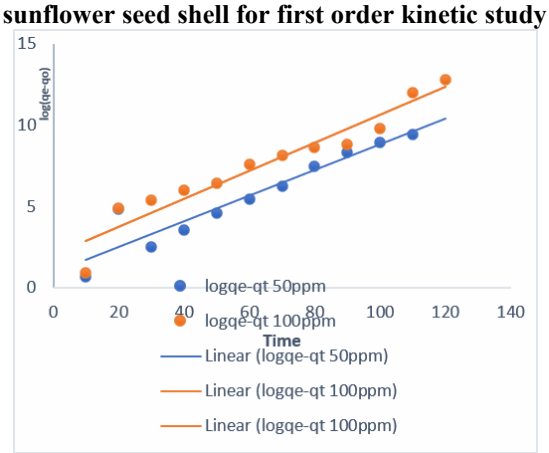

Fig33: Second order plot for MG from Sunflower seed shell

Fig 32 Pseudo first order plot at different concentration of Rhodamine B adsorption onto UBT

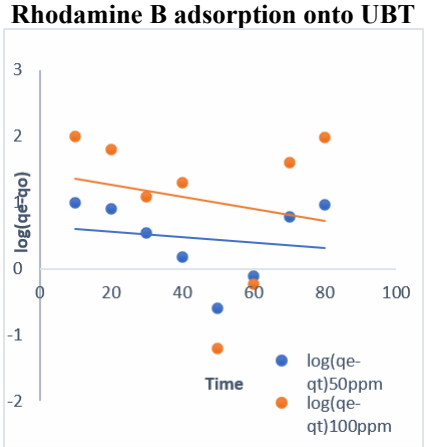

Fig 34: Second order plot of Rhodamine B dye for UBT adsorption :

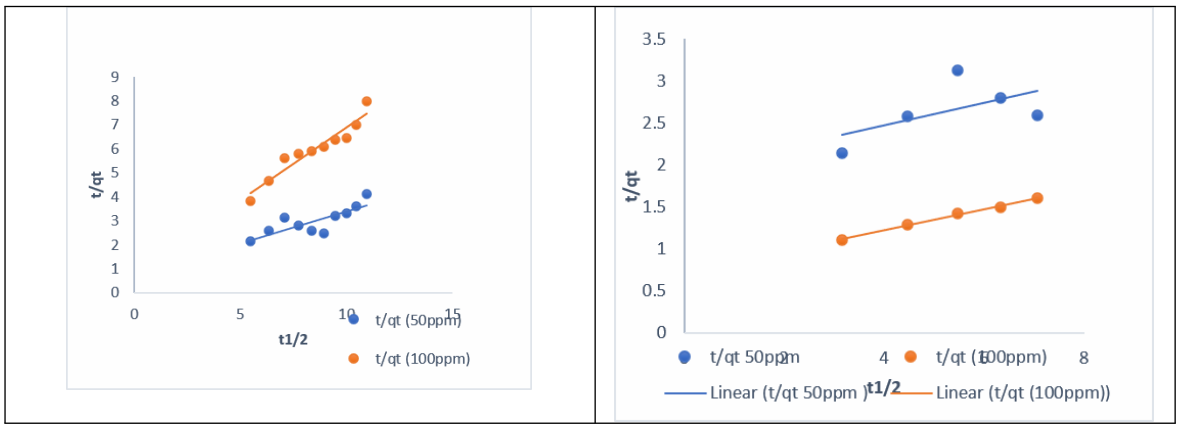

Table 9: **Pseudo-first order kinetics for RDB for UBT:**

	Pseudo first order kinetics			Pseudo second order kinetics		
Dye	K_1	q_e	R^2	K_2	q_e	R^2
,MG 100ppm	0.19892	97.52	0.9256	1.2097	1.6474	0.919
50ppm	0.1821	7.5928	0.8979	1.3283	3.7221	0.6605
Rhodamine B dye (100ppm)	0.020727	27.996	0.0365	0.5166	7.4794	0.3329
RhB Dye (50ppm)	0.0096726	4.44483	0.0313	1.3987	7.942	0.9953

Intra-particle diffusion model

In adsorption process, the adsorbed species are most probably transported from the bulk of the solution into the solid phase through intra-particle diffusion, which is the rate limiting step. In addition, there is a possibility of the adsorbate to diffuse into the interior pores of the adsorbent. Weber and Morris proposed linear equation for intra-particle diffusion model, which is given in the following form.

$qt = K_{ipd}\, t^{1/2} + C$

where K_{ipd} is the intra-particle diffusion rate constant (mg g^{-1} min^{-1}) and C is the constant (mg g^{-1}). The intra-particle diffusion rate constant K_{id} and C have been calculated from the slope and intercept of the plot between q_t verses $t^{1/2}$

The intra particle diffusion parameters rate constant ,kd and thickness of boundry layer at 50 aand 100mg/L of Mg and RB were also evaluated from the plot of qt versus t1/2 (fig 35 ND 36) and are listed in table. According to well known intra-particle diffusion model, if the plot of qt versus t1/2 gives a straight line, thenthe adsorption process is controlled by intra particle diffusion ,while ,if the data exhibits multi-linear plots,then two more ssteps influence the adsorption process [46,47] In the present study, the plots presents linearitty not passing thrrough origin (fig 35 and 36), indicating the aadsorrption was not totaally controlled by intra paarticle diffusion. The values of intra intra particle diffusion, rate constant,kd linearaly increses with increase in concentraation of MG and RB, indicating that with increaase in concentraataion, the diffusion rate are at solid -liquid interface increses. This indicates that intraa paarticcle diffusion mecchanism was involves in adsorption of MG, RB on activated charcoal of sunflower seed shell and used black tea onto activated charcoal. the deviation of straight lines from the origin indicates that the intra-particle diffusion is not the sole rate -ccontrolling mechaanissm [16,37]. The intraparticle rate diffusion constant ,kd and thickness of boundry layer shown in table10

Fig 33(a): Intraparticle diffusion of MG on activated charcoal prepared from Sunflower seed shell	**Fig 33(b): Intraparticle diffusion of RB on activated charcoal prepared from UBT**

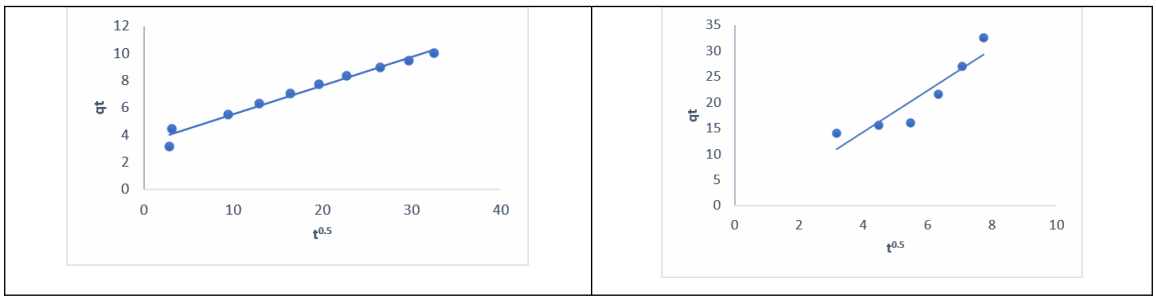

Table 10: Values for K_{ipd} for Intraparticle diffusion for sorption of Azo dyes on Activated charcoal

Azo dye	Co	K_{ipd}	I	R^2
MG	50ppm	0.2105	3.4001	0.975
Rhodamine B dye	50ppm	3.9916	1.6698	0.845

The graph for MG and Rhodamine B dye shows linear graph. The regression coefficient values and intraparticle diffusion values are shown in the table. High values of regression coefficients (R^2) indicate for MG dye adsorption is more as compare to RhB dye.

III. Conclusion:

Porous activated carbon was synthesized using sulphuric acid and characterized by FTIR and scanning electron microscopy (SEM). The solution's pH significantly affects the adsorption capacity of sulphuric acid activated carbon (UBT and SSS) for both dyes. Optimal adsorption conditions for Melachite green (MG) and Rhodamine B (RhB) occur at pH 2 and pH 9, respectively. Equilibrium data were evaluated using Langmuir, Freundlich, and Temkin isotherm models. Langmuir fits MG and RhB dyes, while Freundlich shows superior fit due to the heterogeneous nature of UBT and SSS. Maximum monolayer adsorption capacities for MG and RhB are 222.22 mg and 97.082 mg per gram at 298 K. Batch adsorption kinetics reveal that dye adsorption follows pseudo-second order kinetics at two concentrations, indicating chemisorption as the rate-limiting step.

References:

[1]. Asgari Et. Al., 2012; Dogan Et Al., 2004, Adsorption Kinetics And Isotherms For The Removal Of Rhodamine Dye And Metal,Arabian Journal Of Chemistry,2016.
[2]. A.N. Kagalkar, U.B. Jagtap, J.P. Jadhav, V.A. Bapat, S.P. Govindwar, Bioresour. Technol, Biochemical Degradation.
[3]. B. Gozmen, B. Kayan, A.M. Gizir, A. Hesenov, J. Hazard. Mater.)
[4]. Boyjoo Y, Choueib A, Zhu Z 2005, Jorf S, Barzegar G, Ahmadi M, Soltani RDC, Takdastan A, Saeedi R, Abtahi M (2016).
[5]. Bansal, R.C., And Goyal, M.,. Activated Carbon Adsorption. CRC Press,2005.
[6]. Carbon Fareeda Hayeeye*, Maimoon Sattar, Surajit Tekasakul, And Orawan Sirichote Adsorption Of Rhodamine B On Activated Carbon Obtained From Pericarp Of Rubber Fruit In Comparison With The Commercial Activated. Department Of Chemistry, Faculty Of Science, Prince Of Songkla University, Hat Yai, Songkhla, 90112 Thailand. Received 15 May 2013; Accepted 6 December, 2013
[7]. Deshpande, A. V., & Kumar, U. (2002). Effect Of Method Of Preparation On Photophysical Properties Of Rh-B Impregnated Sol–Gel Hosts. Journal Of Non-Crystalline Solids, 306, 149–159.10.1016/S0022-3093(02)01054-2
[8]. Foo, K.Y., Hameed, B.H., A Review Of Activated Carbon Adsorption, Chemical Engineering Journal, 156, 2–10. (2012).
[9]. Dubinin, M. M., & Radushkevich, L. V. (1947). Equation Of The Characteristic Curve Of Activated Charcoal. Proceedings Of The National Academy Of Sciences, 55, 331–337.
[10]. Dogan M, Alkan M. Adsorption Kinetics Of Methyl Violet Onto Perlite. Chemosphere. 2003;50:517
[11]. D.K. Gardiner, B.J. Borne, J. Soc. Photodegradation Dyers Colour
[12]. T. Robinson, G. Mcmullan, R. Marchant, P. Nigam, Bioresour. Technol. 77 (2001) 247–255)
[13]. K.S. Paramakalyani, N. Balasubramanian, C. Srinivasakannan, Electrocoagulation, Chem. Eng El-Geundi MS. Homogeneous Surface Diffusion Model For The Adsorption Of Basic Dyestuffs Onto Natural Clay In Batch Adsorbers Adsor. Sci. Technol. 1991;8:217.
[14]. Guo, Y.; Rockstraw, D.A. Activated Carbons Prepared From Rice Hull By One-Step Phosphoric Acid Activation. Microporous Mesoporous Mater., , 12–19. 100,2007.
[15]. Ghosh And Bhattacharyya, 2002, Avom Et Al, 1997.
[16]. P. Saha, Water Air Soil Pollut., 213, 287-299 (2010). 49. M. A. Tofighy, T. Mohammadi, J. Hazard. Mater., 185, 140-147 (2011). The Intraparticle Rate Diffusion Contant ,Kd And Thickness Of Boundry Layer.
[17]. Jafari S, Zhao F, Zhao D, Lahtinen M, Bhatnagar A, Sillanpää M 2015, Shojaei S, Khammarnia S, Shojaei S, Sasani M 2017)
[18]. Gad, H. M., & El-Sayed, A. A. (2009). Activated Carbon From Agricultural By-Products For The Removal Of Rhodamine-B From Aqueous Solution. Journal Of Hazardous Materials, 168, 1070–1081.10.1016/J.Jhazmat.2009.02.155
[19]. Hameed, B. H. (2008). Equilibrium And Kinetic Studies Of Methyl Violet Sorption By Agricultural Waste. Journal Of Hazardous Materials, 154, 204–212.10.1016/J.Jhazmat.2007.10.010
[20]. Hanafiah, M. A. K. M., Ngah, W. S. W., Zolkafly, S. H., Teong, L. C., & Majid, Z. A. A. (2012). Acid Blue 25 Adsorption On Base Treatedshorea Dasyphylla Sawdust: Kinetic, Isotherm, Thermodynamic And Spectroscopic Analysis. Journal Of Environmental Sciences, 24,261–268.10.1016/S1001-0742(11)60764-X
[21]. Ho, Y. S., & Mckay, G. (1999). Pseudo-Second Order Model For Sorption Processes. Process Biochemistry, 34,451–465.10.1016/S0032-9592(98)001125
[22]. Hu, Y., Guo, T., Ye, X., Li, Q., Guo, M., Liu, H., & Wu, Z. (2013). Dye Adsorption By Resins: Effect Of Ionic Strength On Hydrophobic And Electrostatic Interactions. Chemical Engineering Journal, 228, 392–397.10.1016/J.Cej.2013.04.116

[23]. Jamaludheen, V. & Kumar, B. M. (1999). Litter Of Multipurpose Trees In Kerala, India: Variations In The Amount, Quality, Decay Rates And Release Of Nutrients. Forest Ecology And Management, 115, 1–11.10.1016/S0378-1127(98)00439-3
[24]. J.P. Chen, S. Wu, K.-H. Chong, Carbon, 41, 1979-1986 (2003).
[25]. K.R.Ramakrishna And T. Viraraghavan, Dye Removal Using Low Cost Adsorbents, Water Science Technology,Vol, 36, No.(2-3), 1997 , Pp189-196.
[26]. Kooh, M. R. R., Lim, L. B. L., Lim, L. H., & Bandara, J. M. R. S. (2015). Batch Adsorption Studies On The Removal Of Malachite Green From Water By Chemically Modified Azolla Pinnata. Desalination And Water Treatment. Doi:10.1080/19443994.2015.1065450
[27]. Lagergren, S. (1898). Zur Theorie Der Sogenannten Adsorption Gel Ster Stoffe. Kongl. Svenska Vetenskaps Academiens Handlingar,24, 1–39
[28]. M. R. R., Lim, L. B. L., Dahri, M. K., Lim, L. H., & Sarath Bandara, J. M. R. (2015). Azolla Pinnata: An Efficient Low Cost Material For Removal Of Methyl Violet 2B By Using Adsorption Method. Waste And Biomass Valorization, 6, 547–559.10.1007/S12649-015-9369-0
[29]. Langmuir, I. (1916). The Constitution And Fundamental Properties Of Solids And Liquids. Part I. Solids. Journal Of The American Chemical Society, 38, 2221–2295.10.1021/Ja02268a002
[30]. Mittal, A., Et Al., Adsorption Of Rhodamine B Onto Activated Carbon. Journal Of Hazardous Materials,2010..
[31]. Lim, L. B. L., Priyantha, N., Chan, C. M., Matassan, D., Chieng, H. I., & Kooh, M. R. R. (2014). Adsorption Behavior Of Methyl Violet 2B Using Duckweed: Equilibrium And Kinetics Studies. Arabian Journal For Science And Engineering, 39, 6757–6765.
[32]. Maurya, N. S., Mittal, A. K., Cornel, P., & Rother, E. (2006). Biosorption Of Dyes Using Dead Macro Fungi: Effect Of Dye Structure, Ionic Strength And Ph. Bioresource Technology, 97, 512–521.10.1016/J.Biortech.2005.02.045
[33]. Mishra, G.; Tripathy, M. A. Colourage 1993, 22, 35-38.
[34]. Martin, M. J., Artola, A., Balaguer, M. D. And Rigola, M. (2003) Activated Carbons Developed From Surplus Sewage Sludge For The Removal Of Dyes From Dilute Aqueous Solution. Chem. Eng. J. 94, Pp. 231-239.
[35]. Malik, P. K. (2004) Dye Removal From Wastewater Using Carbon Developed From Sawdust: Adsorption Equilibrium And Kinetics. J. Hazard. Mater. B113, Pp. 81-88.
[36]. Markovska, L.; Meshko, V.; Noveski, V. Korean J. Chem. Eng. 2001, 18, 190-195. Namasivayam, C. And Kavitha, D. (2002) Removal Of Congo Red From Water By Adsorption Onto Activated Carbon Prepared From Coir Pith, An Agricultural Solid Waste. Dyes Pigments 54, Pp. 47-58.
[37]. Namasivayam, C. And Yamuna, R. T. (2005) Adsorption Of Direct Red By Biogas Residual Slurry. Environ. Pollut. 89, Pp. 1-8.
[38]. Markovska, L.; Meshko, V.; Noveski, V. Korean J. Chem. Eng. 2001, 18, 190-195. Namasivayam, C. And Kavitha, D. (2002) Removal Of Congo Red From Water By Adsorption Onto Activated Carbon Prepared From Coir Pith, An Agricultural Solid Waste. Dyes Pigments 54, Pp. 47-58.
[39]. M. A. Tofighy, T. Mohammadi, J. Hazard. Mater., 185, 140-147 (2011.).
[40]. Olugbenga S. B., Idowu A. A., John C. A., Ezekiel O. F. Adsorption Of Methylene Blue Onto Activated Carbon Derived From Periwinkle Shells: Kinetics And Equilibrium Studies, Chemistry And Ecology. 2008, 24 (4), 285 -295.
[41]. Özacar, M., & Şengil, İ. A. (2004). Application Of Kinetic Models To The Sorption Of Disperse Dyes Onto Alunite. Colloids And Surfaces A: Physicochemical And Engineering Aspects, 242, 105–113.
[42]. K.R.Ramakrishna And T. Viraraghavan, Dye Removal Using Low Cost Adsorbents, Water Science Technology,Vol, 36, No.(2-3), 1997 , Pp189-196.
[43]. Santhi, T., Prasad, A. L., & Manonmani, S. (2014). A Comparative Study Of Microwave And Chemically Treated Acacia Nilotica Leaf As An Eco Friendly Adsorbent For The Removal Of Rhodamine B Dye From Aqueous Solution. Arabian Journal Of Chemistry, 7,494–503.10.1016/J.Arabjc.2010.11.008
[44]. Sigma-Aldrich. (2014). Rhodamine B [Material Safety Data Sheet] Version 5.4. Retrieved September 21, 2015,
[45]. Saruchi, Vaneet Kumar, Adsorption Kinetics And Isotherms For The Removal Of Rhodamine B Dye And Pb^{+2} Ions From Aqueous Solutions By A Hybrid Ion-Exchanger, Arabian Journal Of Chemistry 12(3);316-329 2016.(Zhang Et.Al.2009; Chiou And Li2002; Langmuir1918):
[46]. Tavlieva, M. P., Genieva, S. D., Georgieva, V. G., & Vlaev, L. T. (2013). Kinetic Study Of Brilliant Green Adsorption From Aqueous Solution Onto White Rice Husk Ash. Journal Of Colloid And Interface Science, 409, 112–122.10.
[47]. Tsai, S. C., & Juang, K. W. (2000). Comparison Of Linear And Nonlinear Forms Of Isotherm Models For Strontium Sorption On A Sodium Bentonite. Journal Of Radioanalytical And Nuclear Chemistry, 243, 741–746.10.1023/A:1010694910170
[48]. A. Dobrowski, Adv. Colloid Interface Sci. 93 (2001) 135–224)
[49]. J.P. Chen, S. Wu, K.-H. Chong, Carbon, 41, 1979-1986 (2003)
[50]. Kumar, T.S.M.; Rajini, N.; Reddy, K.O.; Rajulu, A.V.; Siengchin, S.; Ayrilmis, N. All-Cellulose Composite Films With Cellulose Matrix And Napier Grass Cellulose Fibril Fillers. Int. J. Biol. Macromol. 2018, 112, 1310–1315.
[51]. Mittal, A., Et Al., Adsorption Of Rhodamine B Onto Activated Carbon. Journal Of Hazardous Materials,2010..
[52]. Preparation And Evaluation Of An Effective Activated Carbon From White Sugar For The Adsorption Of Rhodamine B Dye
[53]. Wang, S., And Zhu, Z.H.,. Effects Of Functional Groups On Adsorption Of Dyes. Dyes And Pigments,2007.
[54]. W.J. Weber, J.C. Morris, J. Sanit. Eng. Div., 89, 31-60 (1963).
[55]. Shojaei S, Khammarnia S, Shojaei S, Sasani M (2017), Removal Of Reactive Red 198 By Nanoparticle Zero Valent Iron In The Presence Of Hydrogen Peroxide. J Water Environ Nanotechnol 2(2):129–135
[56]. Seyyed. A.M, Bahram C., Ali A., Mohammad D., Ararvismoteval, Mehdi S., Faramarz A., Mansour G., Zhaleh N. Mohammed., A.K. Regional Article Published,10 June 2021.
[57]. Foo, K.Y., Hameed, B.H., A Review Of Activated Carbon Adsorption, Chemical Engineering Journal, 156, 2–10. (2012).
[58]. Babel, S., Kurniawan, T.A., Low-Cost Adsorbents For Heavy Metals Uptake From Contaminated Water, Journal Of Hazardous Materials, 97, 219–243(2003).
[59]. Demirbas, A. (2008), Heavy Metal Adsorption Onto Agro-Based Waste Materials, Journal Of Hazardous Materials, 157, 220–229, (2008).
[60]. Ioannidou, O., Zabaniotou, A., Agricultural Residues As Precursors For Activated Carbon, Renewable And Sustainable Energy Reviews, 11, 1966–2005, (2007)
[61]. Gupta, V.K., And Suhas, Application Of Low-Cost Adsorbents For Dye Removal. Journal Of Environmental Management,2009.
[62]. Mittal, A., Et Al., Adsorption Of Rhodamine B Onto Activated Carbon. Journal Of Hazardous Materials,2010..
[63]. 63. Z. Zhang, Ian M. O'Hara, Geoff A. Kent, William O.S. Doherty, Comparative Study On Adsorption Of Two Cationic Dyes By Milled Sugarcane Bagasse, Ind. Cr